 #4159

Building ventilation
Analysis of air circulation through a building

VALIDATION OF MODEL FOR DIFFERENT WIND INDICES AND OPENINGS IN THE BUILDING ENVELOPE

Joëlle Passard

This paper by Joëlle Passard was carried out at the Laboratorie d'Etude des Systèmes Thermiques et Energétiques, LESTE, directed by Professor Peube of the University of Poitiers, in collaboration with CSTB Nantes and provides a detailed account of the development of a numerical model for estimating the airflow rates through openings and cracks in the building envelope.

L'étude de Joëlle Passard a été effectuée au Laboratoire d'Etude des Systèmes Thermiques et Energétiques, le LESTE, dirigé par le Prof. Peube de l'Université de Poitiers, en collaboration avec le CSTB – établissement de Nantes, et donne un compte rendu détaillé du développement d'un modèle numérique pour l'évaluation des débits d'air à travers ouvertures et fissures dans l'enveloppe des bâtiments.

Nomenclature

A : State matrix of the aeraulic system
$\mathscr{A}$: State matrix of the aeraulic linear system
B : State-input matrix of the aeraulic system
$\mathscr{B}$: State-input matrix of the aeraulic linear system
C : Output-state matrix of the aeraulic system
$\mathscr{C}$: Output-state matrix of the aeraulic linear system
$\overline{c}$: Mean pressure coefficient
C_k : Aeraulic capacity of a zone k (m^3/Pa)
D : Output–input matrix of the aeraulic system
$\mathscr{D}$: Output–input matrix of the aeraulic linear system
D_o : Hydraulic diameter of an opening (m)
D_h : Hydraulic diameter of a zone in direction of flow (m)
F : State matrix of the reduced model or section of a zone
F_o : Section of an opening (m^2)
F_1 : Characteristic section before the opening (m^2)
F_2 : Characteristic section after the opening (m^2)
G : State-input matrix of the reduced model
H : Output-state matrix of the reduced model
J : Quadratic criterion of optimization
K : Permeability of an opening (m^3/s under 1 Pa) or output–input matrix of the reduced model
L : Characteristic length of a zone (m) or aggregated matrix
l : Thickness of an opening (m)
L_0 : Aggregated matrix
M : Eigenvector matrix
m : Dimension of the aeraulic system
m_c : Number of columns of the plan cell
m_l : Number of lines of the plan cell
m_r : Dimension of the reduced model
N : Square matrix
P : Pressure (Pa)
$\mathscr{P}$: Matrix of energy in steady state
Q : Airflow rate (m^3/s)
$\overline{R}_{kl}$: Permeability of an opening between two zones k and l (m^3/s under 1 Pa)
Re : Reynolds Number
T : Temperature (°C)
t : Time (s)
U : Input vector of the aeraulic model in steady state
V : Wind speed (m/s)
V_k : Volume of a zone k (m^3)
W_0 : State matrix in steady state
w_0 : Speed of flow through opening (m/s)
w_1 : Speed of flow before opening (m/s)
w_2 : Speed of flow after opening (m/s)
X : State vector of the aeraulic system
$\overline{X}_{kl}$: External pressure of a zone k
x : A dimensional State vector ($X/0{,}5\ \rho\ V^2$)
Y : Output vector of the aeraulic system
$\hat{Y}$: Output vector of the reduced model
y : Adimensional output vector of the aeraulic system (Y/V)
Z : State vector of the reduced model
z : Height (m)

Greek letters

α : Coefficient of sub-relaxation
α_{kl} : Mean Coefficient of the permeability between two zones k and l
Γ : State-input matrix modal basic
ΔP : Difference of pressure (Pa)
ΔT : Difference of temperature (°C)
ξ : Singular drop in pressure coefficient of an opening
ζ_l : Linear drop in pressure coefficient in a zone
θ : Incidence of wind (°)
λ : Eigenvalue (s^{-1}) or lineic drop in pressure coefficient of an opening
Λ : Diagonal eigenvalue matrix
μ : Dynamic viscosity of air (kg/m.s)
π_o : Perimeter of an opening (m)
ρ : Air density (kg/m^3)
Ω : Output-state matrix in modal basic
χ : State vector in modal basic

Introduction

Over the past 20 years, the energy crisis has been forcing designers to optimize energy use in buildings. Of the principal elements which govern human comfort, air temperature, humidity and air movement, the latter is the only one which can be significantly controlled without substantial energy use (ref. 1). But with the important improvement in methods of assessing the thermal performance of buildings, the lack of a satisfactory method of evaluating ventilation rates becomes an acute problem. For example, the energy losses by ventilation during cold periods of temperate climate can reach up to 30 per cent of the total heat losses in buildings.

Prediction of natural ventilation, infiltration and air movement in buildings is difficult for two principal reasons. Firstly, the physical relationships that govern the movement of air through a building are non-linear. Secondly, the airflows are directly induced by the interaction between wind (turbulent phenomenon characterized by its speed and direction) and building within a cluster of buildings (refs 2, 3).

On the other hand, a study of climate conditions shows that there is an appropriate time and place for the effective use of natural air movement.

The combination of all these factors makes a precise evaluation of airflows a practical impossibility. However, we choose to represent the mean airflow through each opening by a model which relates the external mean pressure distribution on building walls to the inner air circulation.

In this paper the model will not take fluctuating forces into account. In building surroundings, the effects on three-dimensional bluff bodies immersed in a turbulent boundary layer are given by pressure coefficients: scalar measures on a surface, reported to the reference wind speed. In this manner we obtain a realistic assessment of ventilation rates in buildings. But we have to recognize that the practical aspects of such a model are limited.

First of all, we are going to study the physics of infiltration and the method for building the theoretical model. Then we will propose a modal analysis of this model, which will allow us to reveal some properties of this system according to the laws of physics.

We will also examine the possibility of reducing the model by aggregation method. This can be a substantial aspect of integrating this model in a more general description of thermal performance of buildings.

Physics phenomena description

Air infiltration mechanism

There are two natural energy sources which are used to promote airflow through buildings:

1. Pressure differences due to air density variations created by differences in air temperature, referred to as the stack effect, and
2. Pressure differences due to distribution of wind pressures on building surfaces.

Pressure differences from the stack effect and wind pressure distribution can act simultaneously, the effective pressure difference being their algebraic sum.

$$\Delta P = \Delta P_{th} + \Delta P_v \quad (1)$$

$$\Delta P_{th} = -\rho g \beta z (T_i - T_e) \quad (2)$$

$z = h - h_o\,(m)$: h_o is the height at which inner and external pressures are equal, where

$\beta = 1/T_i$: air is assumed to be a perfect gas ($°K^{-1}$)
T_i: inner temperature (°K)
T_e: external temperature (°K)
g: gravitational acceleration (m/s^2)

$$\Delta P_v = \bar{c} 0.5 \rho V^2 \quad (3)$$

where

$\bar{c}$: mean pressure coefficient
ρ: density of air (Kg/m^3)
V: reference wind speed (m/s)

Pressure differences due to wind have generally a dominant effect on airflow rates. However, in certain cases the two phenomena are equivalent. So we have to take stack effect into account. In this paper, we consider only airflow through buildings caused by wind forces.

Airflow definition

In literature, the airflow rate resulting from a pressure difference is generally written as:

$$Q = K^* \Delta P^n \quad (4)$$

K^* and n are parameters which depend on the geometry of opening and characteristics of flow through opening. The parameter n lies between 0.5 and 1.0 and usually has the value of 0.65.

In his work (ref. 4), R.M. Aynsley lets $n = 0.5$ for large openings and large Reynolds numbers ($2000 < Re < 10\,000$).

In our case, we will choose smaller openings and consequently a smaller Reynolds number ($100 < Re < 1000$), so we prefer to use the Darcy law, which seems to be more appropriate:

$$Q = K \Delta P \quad (5)$$

where K, the permeability, is a function of airflow rate through openings. The calculation of permeability is

given in Appendix 1, from the results of 'Memento des pertes de charge' (ref. 5).

$$K = 2F_o 2/\xi\rho Q \quad (6)$$

F_o: section of the opening (m^2)
ξ: drop in pressure coefficient

From these expressions (5 and 6), the airflow through openings can be characterized for any geometries and flow conditions.

However, we must make reservations. The results of Memento are obtained experimentally in an orifice calibration tunnel. It would be interesting to obtain equivalent results realized in more realistic conditions. In Figure 1 we can compare the realistic conditions of flow through and around buildings with the experimental conditions of Memento.

Presentation of the aeraulic model

The model determines the flow rates through a partially opened enclosure, subjected to an external boundary layer flow.

Experimentation

Before we study the numerical model, it is important to recall the essential role played by experimental modelling, such as simulations in wind tunnels (ref. 4).

This aeraulic model is a complementary option, which allows us a study of a diversity of configurations at a reasonable cost, but this cannot be realized without the contributions of experimentation.

Indeed, experimentation is the only method that gives us the pressure distribution on building walls for different wind conditions (refs 4, 6). It was noted that these results were obtained for non-porous models and were directly used for buildings with small openings. We assumed that openings did not disturb the pressure distribution. Finally, experimentation has been allowing us to understand a good number of physics phenomena stemming from interactions between buildings and external airflow.

Numerical model – basics

The building is compared to a multizone cell with small openings. The working hypothesis of small openings permits us to consider the pressure defined in each zone. The electric–aeraulic analogy introduces the notion of network, in which each zone at a defined pressure is

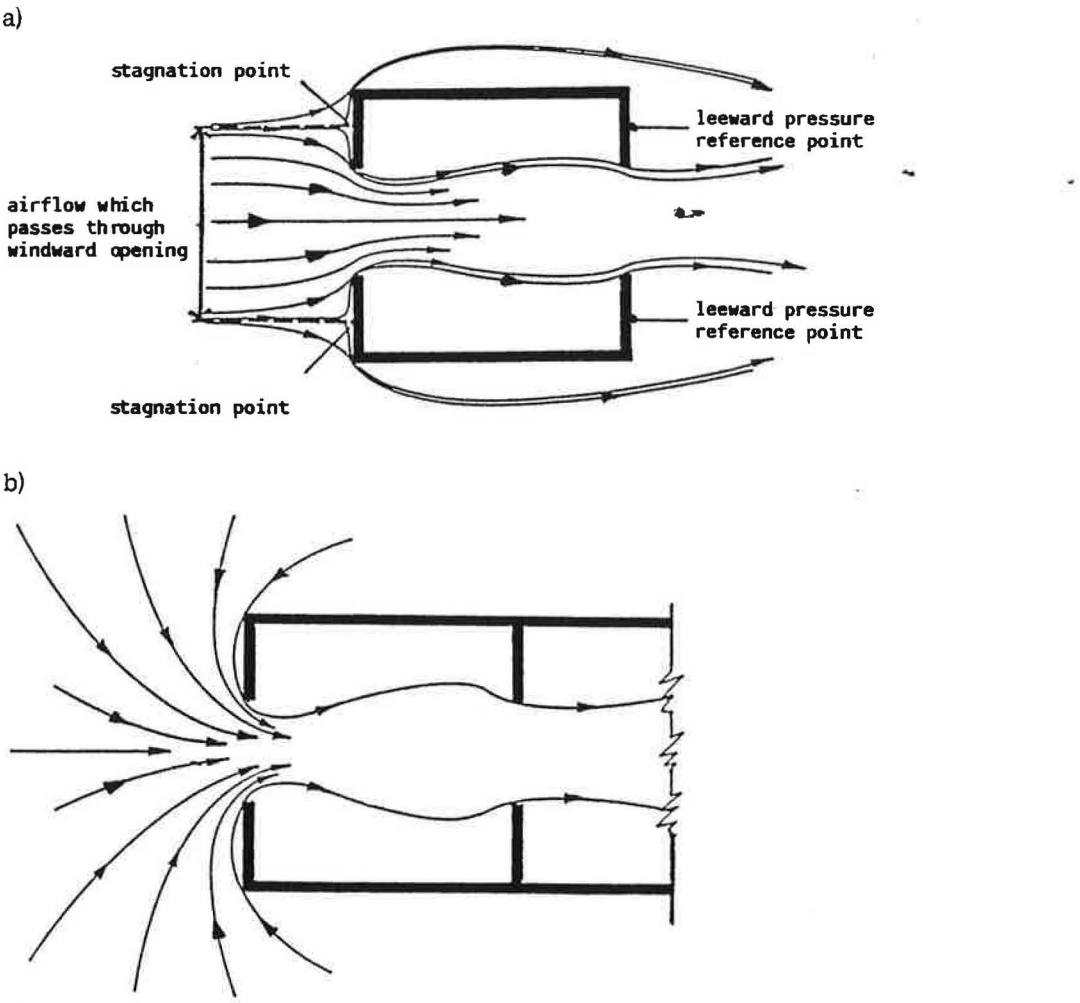

Fig. 1. (After Aynsley /4/) a) Typical airflow through and around a simple building indicating similarity to orifice flow in a pipe. b) Typical airflow pattern at entry to orifice calibration tunnel

represented by a network junction in communication with other junctions. Here the electric-aeraulic analogy is a simple intellectual aid from which our reasoning is derived.

The non-linear, time system of equations, discrete in space, is obtained:

$$\frac{d}{dt} X(t) = A\,X(t) + BU(t)$$
$$Y(t) = C\,X(t) + DU(t) \quad (7)$$

$X(t)$ is the m dimension state vector of the system. Its components are the pressure on each network junction.

A is an m dimension square matrix, whose band shape is due to the distribution of openings. Moreover, A is a symmetrical matrix due to the permeability of the opening which has the same value for the outgoing and incoming flow rate from one zone to the next

$$.A_{kk} = -\sum_{\text{k'neighbours}} \bar{R}_{k,k'}/C_k \quad (8)$$

$\bar{R}_{k,k'}$ is the permeability of the opening between zones k and k'. C_k is the aeraulic capacity of zone k.

If zone k communicates with zone l then:

$$.Akl = \bar{R}_{k,l}/C_k \quad (9)$$

Else $\quad .A_{k,l} = 0.$

The system is dependent on external perturbations represented by the r dimension input vector $U(t)$. The components of product $B.U(t)$ contain the external pressure.

If zone k has i external openings:

$$B'_k = \sum_i \bar{X}_{k,li}.\bar{R}_{k,li}/\mathscr{C}_k \quad (10)$$

$$B' = B\,U(t) \quad (11)$$

$\bar{X}_{k,li}$ represents the external pressure around the opening.

Y is the output vector of which the q components are the flow rates through each opening.

According to the flow definition (2.5), matrices C and D are written as:

$$.C_{n,k} = -\bar{R}_{k,l} \quad (12)$$

If zone l is next to zone k then:

$$.C_{n,l} = \bar{R}_{k,l} \quad (13)$$

otherwise stated as:

$$.C_{n,l} = 0$$

If $\bar{R}_{k,li}$ represents an external opening of the zone k then:

$$.D'_n = \bar{X}_{k,li}.\bar{R}_{k,li} \quad (14)$$

$$.D' = D\,U(t) \quad (15)$$

For each value of n, a number which represents the flow rates, there are only two suffixes k and l which are previously mentioned in the above formulae.

This mathematical formulation of aeraulic phenomena in buildings allows us to study properties and solutions of the system.

The solution of model equations

At first sight, there is no obvious analytical solution to the system of equations (7) for two reasons. The first, as mentioned previously, concerns the non-linearity of the system. Indeed, the matrix (A, B, C, D) coefficients are non-constant because of permeability expression $\bar{R}$, which depends on flow conditions through openings. On the other hand, the pressure $X(t)$ and flow rate $Y(t)$ vectors are functions of time conditioned by the input vector $U(t)$.

Linearization of system

Here we tackle the problem at steady state. The effect of time will be considered later.

For a given wind speed profile which characterizes a type of wind, the distribution of pressure coefficients on building walls stays the same for a certain range of reference wind speeds. So the external pressure can be written as:

$$\bar{X} = \bar{c}.\tfrac{1}{2}\rho V^2 \quad (16)$$

The linearization of system on a speed range are based on two assumptions which are checked by calculations:

1. For small openings ($100 < Re < 1000$), we assume that permeability is inversely proportional to flow rates through itself (Fig. 2).

$$\bar{R}_{kl} = \alpha_{kl}/Y_n \quad (17)$$

with α_{kl} constant on a given speed range.

2. We also assume that the pressure on each zone can be written as:

$$X_k = x_k.\tfrac{1}{2}\rho\,V^2 \quad (18)$$

with x_k constant on a speed range.

The system of equations is homogenized:

$$\begin{cases} 1/V\,\bar{A}\,x + V\bar{B} = 0 \\ Y = V(\bar{C}\,x + \bar{D}) \end{cases} \quad (19)$$

The linearization means the solution is not dependent on the speed for a well-chosen speed range. The adimensional system is written:

$$\begin{cases} 1/V\,\bar{A}\,\underline{x} + V\bar{B} = 0 \\ y = \bar{C}\,x + \bar{D} \end{cases} \quad \text{with } y = Y/V \quad (20)$$

$\bar{A}$, $\bar{B}$, $\bar{C}$, $\bar{D}$ are constant coefficient matrices, arithmetic averages on a speed range of the matrices $V.A$, $1/V.B'$, $0{,}5\,\rho\,V\,C$ and $1/V.D'$.

Transient period – steady state

By construction, the linear symmetric band matrix A has distinct real eigenvalues. The aeraulic phenomena are essentially dissipated. So we deduce that eigenvalues are

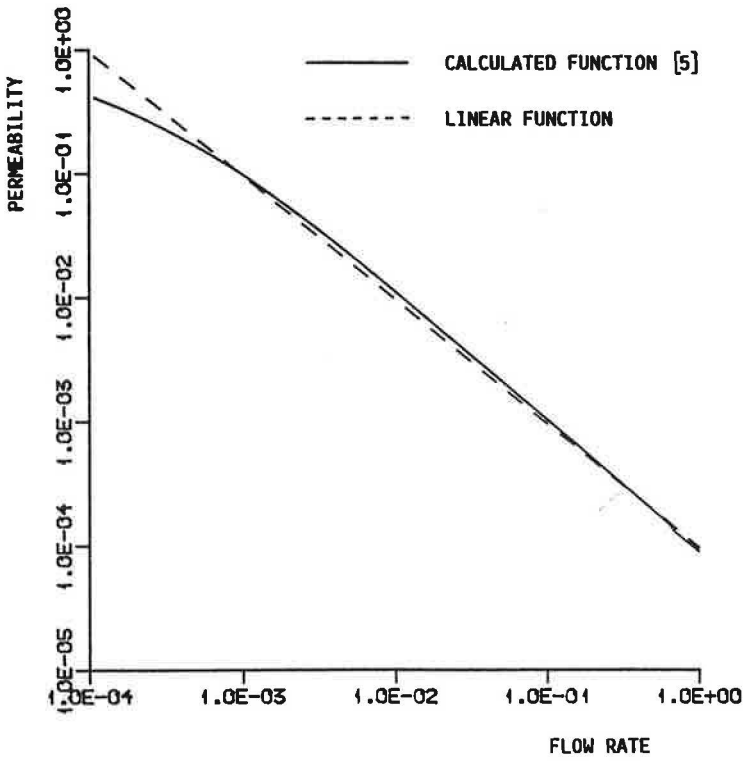

Fig. 2. Permeability function: Opening surface $F_o = 9.10^{-3} m^2$

all negative and that a steady state follows transient period.

A numerical estimation of the model specific times, realized for flow rates about 10^{-3}, 10^{-2} m^3/s (values representative of small openings in our case), gives us values of about 10^{-1} to 10^{-2} s.

Wind specific times are about 10 s and are much larger than those of the aeraulic model. So we deduce that the building behaves like a follower system and takes the least external pressure shock into account. The transient period will be negligible and the steady state is obtained almost instantaneously. The linear system in steady state is written as:

$$\begin{cases} \mathcal{A}X + \mathcal{B}U = 0 \\ Y = \mathcal{C}X + \mathcal{D}U \end{cases} \qquad (21)$$

In that case X,Y and U are no longer dependent on time and U components weight the r system inputs.

Now let us examine some typical results of the model before we investigate the modal system analysis.

Example of ventilation simulation in buildings

For assessing flow rates in buildings, we have conceived an application program named 'AERA', whose principle is explained in Appendix 2. With a simple example, the results of the modelling are presented. A nine-zone cell with four openings by zone is taken. Geometric characteristics are the same for each zone and can be modified according to the needs of the user.

One aim of this work is to be an aid for building designers. So we make a specific effort to represent model results graphically (Fig. 3: m = 9, $F_o = 9.\ 10^{-3}\ m^2$, $V = 15$ m/s, $\theta = 0°$).

Air ambient characteristics

T	inner temperature	20°C or 293°K
ρ	air density	1.21 kg/m^3
μ	dynamic viscosity	1815.10^{-5} Pl

Note that we do not take differences between inner and external air characteristics into account, because the error made on results is negligible.

Characteristics of a standard zone

V_k	standard volume	48 m^3
L_k	characteristic length	2 m
C_k	aeraulic capacity	$3.37\ 10^{-4}$ m^3/Pa

Inner characteristics of the wall that has the opening

Li	width	4 m
Hi	height	3 m
Fi	surface	12 m
D_{hi}	hydraulic diameter	3.43 m

Opening characteristics

F_o	surface	$9\ 10^{-3}\ m^2$ (0.9×0.01 m)
D_o	hydraulic diameter	$2\ 10^{-2}$ m
l_o	thickness	$5\ 10^{-2}$ m

We notice in Figure 3 the symmetric distribution of flow rates in relation to the building's aerodynamic axis. It is the result of a symmetric pressure distribution (wind incidence $\theta = 0°$) and a uniform geometric configuration of the cell (zones and openings are the same). The pressure distribution has been chosen from CSTB works (ref. 6).

In the cell, we can observe good ventilation for windward zones against low ventilation in central and leeward zones. The short-circuit phenomenon, which can be observed in corner zones, is responsible for the low ventilation into the cell. This is confirmed by another example (Fig. 4: m = 15, $F_o = 9.\ 10^{-3}\ m^2$, V = 15 m/s, $\theta = 0°$).

In Figure 4, there is no opening on lateral walls. So the short-circuit effect disappears and there is no transverse flow rate. The building is uniformly ventilated in aerodynamic axis direction.

These two examples show that pressure distribution (wind incidence θ) and repartition of openings are important factors, so we are going to study their influence in the modal structure of our aeraulic model.

Modal analysis of the system (ref. 7)

We recall that we work with the linear steady-state system

$$\begin{cases} \mathscr{A}X + \mathscr{B}U = 0 \\ Y = \mathscr{C}X + \mathscr{D}U \end{cases} \tag{22}$$

and that linearization is realized on a wind speed range.

The specific regular shape of the external distribution of pressures surrounding the building (Figs 3 and 4) influences the modal structure of the system. We will research dominant regular modes and more agitated modes which are less important. We are also going to study how some parameters modify the modal structure of the system.

Characteristic modes of the system

When the system is written in modal basic, we obtain the characteristic modes:

$$X = M_\chi \tag{23}$$

$$\begin{cases} \Lambda\chi + \Gamma U = 0 \\ y = \Omega\chi + \mathscr{D}\chi \end{cases} \tag{24}$$

$$\left.\begin{aligned} \Lambda &= M^{-1}\,\mathscr{A}M \\ \Gamma &= M^{-1}\,\mathscr{B} \\ \Omega &= \mathscr{C}.M \end{aligned}\right\} \tag{25}$$

M is the eigenvector matrix such that:

$$M = /VM_1, VM_2, \ldots, VM_m/ \tag{26}$$

where VM_k is the k^{th} eigenvector associated with the k^{th} eigenvalue λ_k of the diagonal matrix Λ.

The basic change is given by Equation (23). This relation for each component is written as:

$$X_k = \sum_{l=1}^{m} M_{kl}\,\chi_l \tag{27}$$

The system state in each zone appears like a linear combination of the vector χ components. We deduce that coefficients $M_{k,l}$ represent the contribution of l^{th} mode in the k^{th} zone. The contribution of each mode l is weighted by the component χ_l which informs us about the predominance of the mode.

For a better understanding, we have represented the contributions of the nine modes of the first example (Fig. 5). Note that this representation is available for a given wind speed range. Add to this graphic representation the eigenvalues λ and the associated eigenvector χ components:

Eigenvalues	**Vector χ**
$-1.67\ 10^2$	$-7.0\ 10^{-2}$
$-1.42\ 10^2$	10^{-9}
$-1.0\ 10^1$	$-8.29\ 10^{-1}$
$-8.10\ 10^1$	$6.7\ 10^{-2}$
$-9.97\ 10^1$	$-1.45\ 10^{-1}$
$-4.61\ 10^1$	$7.4\ 10^{-2}$
$-5.11\ 10^1$	10^{-9}
$-2.47\ 10^1$	10^{-8}
$-2.63\ 10^1$	$-4.89\ 10^{-1}$

Observing these numerical data, we notice that all the eigenvalues are negative and correspond to the specific time of the system previously calculated. So the system is well spread and we have been justified in neglecting the transient period.

The principal aim of the above listing is to show the different weighting of each mode. It is obvious that each mode has a different influence on the system.

For this example, there are three modes, numbers 2, 7 and 8, which have very low weighting and are negligible. These modes are all antisymmetrical in relation to the aerodynamic axis (Figure 5). Recalling the symmetric geometric configuration of the system, we understand that this one is degenerate. m_d modes are sufficient to describe the model:

$$m_d = m - m_c/2 \cdot m_l \qquad (m_c \text{ even})$$

$$m_d = m - (m_c - 1)/2 \cdot m_l \qquad (m_c \text{ uneven})$$

where m_c is the number of columns and m_l the number of lines in relation to the building ventilation axis.

If the symmetry is broken (wind incidence $\theta \neq 0°$ and/or opening repartition is non-uniform), then the degeneration phenomena of the characteristic states of system disappear.

From vector χ components and the graphic representa-

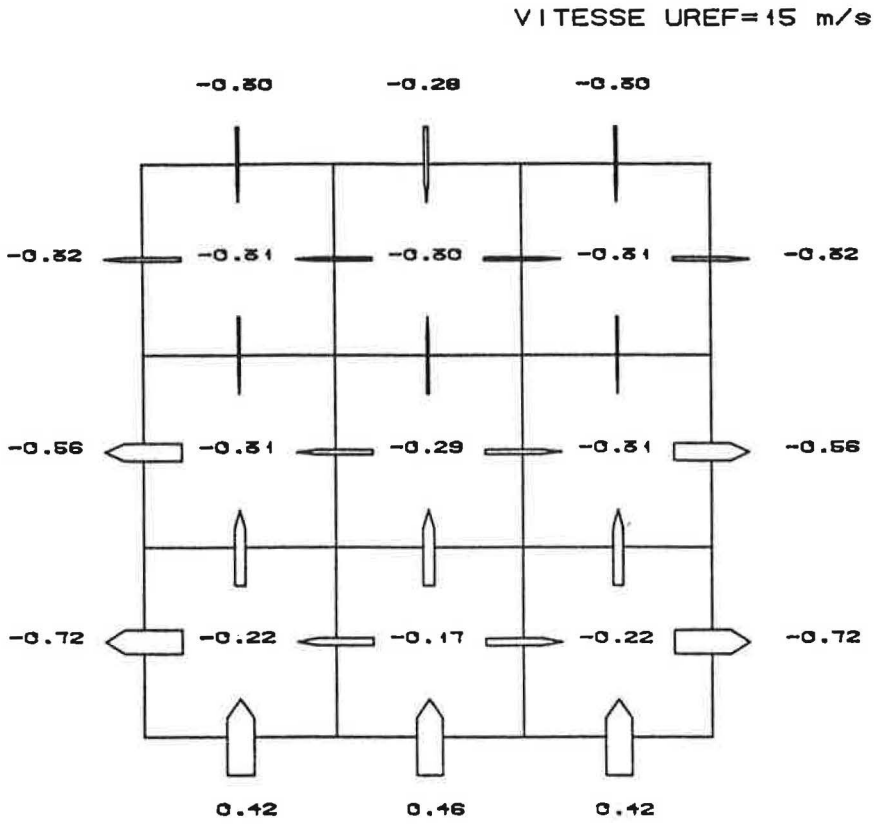

Fig. 3. The airflow distribution in a nine-zone system $\theta = 0^{\circ}$, V = 15 m/s, $F_o = 9.10^{-3} m^2$

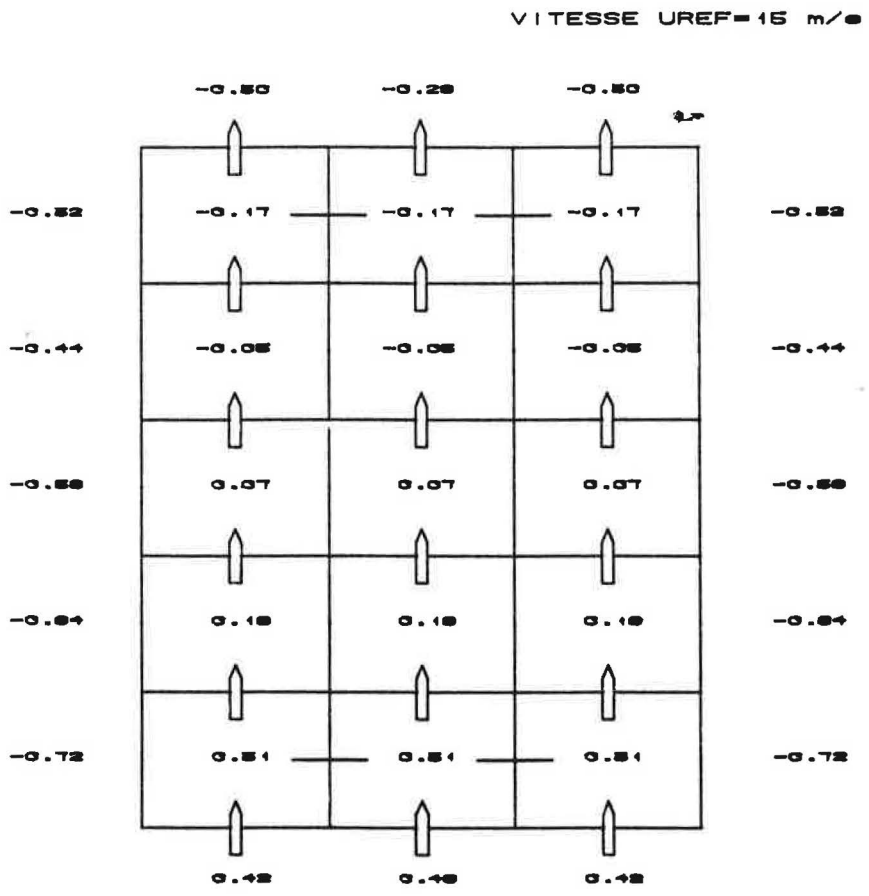

Fig. 4. The airflow distribution in a fifteen-zone system, without lateral openings $\theta = 0°$, V = 15 m/s, $F_o = 9.10^{-3} m^2$

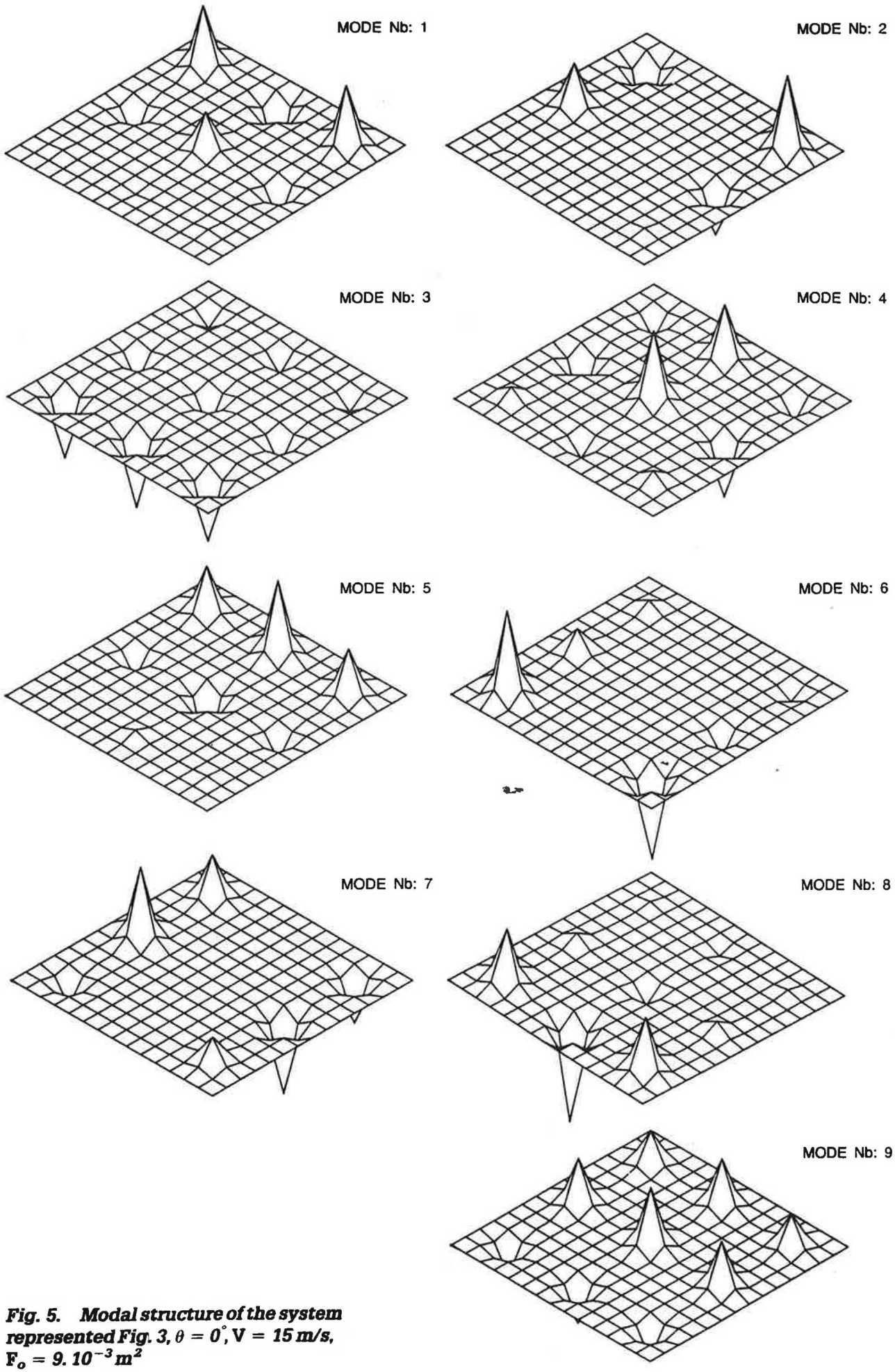

Fig. 5. Modal structure of the system represented Fig. 3, $\theta = 0^{\circ}$, V = 15 m/s, $F_o = 9.10^{-3} m^2$

tion (Fig. 5), we observe that the third mode is dominant. It is symmetric and regular; there is no change of sign in its representation. This mode characterizes the flow through the cell.

The other more agitated symmetric modes (many changes of sign in their representation) are less important but non-negligible. In the second example (15-dimension model represented in Fig. 4), this phenomenon is more pronounced. Indeed the dominant mode has a weighting which is $2\text{–}10^5$ times those of the other symmetric modes.

Now we have to examine the influence of certain parameters on the modal structure of the system.

The influence of uniform modification of openings

Suppose the surfaces of openings are all ten times larger: $F_o = 9.\ 10^{-2}$, $V = 15$ m/s, $\theta = 0°$ (Fig. 6). Consequently the permeability of openings and thus the matrices $\mathcal{A}$, $\mathcal{B}$, $\mathcal{C}$, $\mathcal{D}$ coefficients are multiplied by a same coefficient $\beta \# 10$. The new system is written as:

$$\begin{cases} \beta(\mathcal{A}X^* + \mathcal{B}U) = 0 \\ Y^* = \beta(\mathcal{C}X^* + \mathcal{D}U) \end{cases} \tag{28}$$

The state equation is unchanged. So we obtain the same pressures into the building ($X = X^*$) as in the first example ($F_o = 9.\ 10^{-3}\ m^2$, $V = 15$ m/s, $\theta = 0°$). The modal structure is also unchanged. The flow rate in each opening is multiplied by the coefficient β (Fig. 6 compared with Fig. 3).

We observe the same linear effect as the wind speed varies on a given speed range. Note that these results remain valid if openings are small enough:

Opening dimensions << Building dimension.

The influence of inhomogeneity in the repartition of openings

Here we will not break the symmetry of system. We will just get to know the difference between the inner and external openings.

Let us begin by examining the case for which external openings have a surface ten times larger than inner openings (Fig. 7: $F_{oe} = 9.\ 10^{-2}\ m^2$, $F_{oi} = 9.\ 10^{-3}\ m^2$).

Compare Figure 7 with Figure 6. We notice the lower ventilation in the cell. The short circuit phenomenon is increased and is in part responsible for the low inner ventilation. Except for the leeward zones, pressure coefficients and flow rates are completely modified in the cell.

About the crossing flow rate DEBT, we have a loss of 25%:

$F_{oe} = F_{oi} = 9.\ 10^{-2}\ m^2$	DEBT = 23.53 vol/h
$F_{oe} = 9.\ 10^{-2}\ m^2$, $F_{oi} = 9.\ 10^{-3}\ m^2$	DEBT = 17.51 vol/h

Concerning the modal structure, we also have important modifications (Fig. 8). At first, the contribution of each mode is very localized in space (example: modes 4 and 5). This is explained by the low interaction between zones into the cell, because of the low inner openings in relation to the external ones. Most exchanges take place with the outside. Now examine the weighting of the different modes.

Eigenvalues	Vector χ
$-5.59\ 10^2$	$-3.4\ \ 10^{-2}$
$-5.31\ 10^2$	10^{-8}
$-5.15\ 10^2$	$-5.01\ 10^{-1}$
$-3.18\ 10^1$	$-3.42\ 10^{-1}$
$-1.01\ 10^2$	$-4.43\ 10^{-1}$
$-6.67\ 10^1$	$-1.74\ 10^{-1}$
$-6.73\ 10^1$	10^{-8}
$1.58\ 10^2$	$-7.24\ 10^{-1}$
$-1.60\ 10^2$	10^{-5}

The three negligible modes always exit. Nevertheless, there is no dominant mode. They have all equivalent weightings.

Now we can study the case for which inner openings are ten times larger than external openings. (Fig. 9: $F_{oe} = 9.\ 10^{-3}\ m^2$, $F_{oi} = 9.\ 10^{-2}\ m^2$.)

Pressure is uniform in the cell. This nine-zone building now looks like one big zone. Compared with the first case (Fig. 3: $F_{oe} = F_{oi} = 9.\ 10^{-3}\ m^2$), inner ventilation is not very different. This can be explained by the short-circuit phenomena, which favour exchanges with the outside. Inner ventilation therefore has to be modified very little.

$F_{oe} = F_{oi} = 9.\ 10^{-3}\ m^2$	DEBT = 2.63 vol/h
$F_{oe} = 9.\ 10^{-3}\ m^2$, $F_{oi} = 9.\ 10^{-2}\ m^2$	DEBT = 2.66 vol/h

Modal structure is unchanged, except that the ratio between the two most important modes is 10^2. Remember that it is 2 in the first example and the dominant mode characterizes the flowing through the cell.

Through this study, the model is in accord with the physics phenomenon. The modal structure analysis reveals dominant and negligible modes. So we deduce that the model can be reduced.

We are going to present a reduction of the model by the aggregation method.

Reduction by linear aggregation

Problem statement (refs 8, 9)

Consider two linear dynamic systems S_1 and S_2, where the dimension of S_1 m is much larger than that of S_2, m_r. The state vectors of these two systems, denoted by X and Z, respectively, under certain conditions satisfy the relationship.

$$Z = LX \tag{29}$$

where L is an $(m_r \times m)$ constant matrix.

S_2 is regarded as a model of S_1. The dynamic structure of S_2 reflects the significant portion of the dynamics of S_1. S_2 is called an aggregated model of S_1.

The concept of aggregation proposed in this paper is shown to be useful in deriving a computationally efficient algorithm for suboptimal controls. The basic idea is to partition the state vector into several subvectors and to construct suboptimal state vector estimates from the subvectors.

Given our linear, multi-input, multi-output system described by the steady-state space equations:

$$\begin{cases} \mathcal{A}X + \mathcal{B}U = 0 \\ Y = \mathcal{C}X + \mathcal{D}U \end{cases}$$

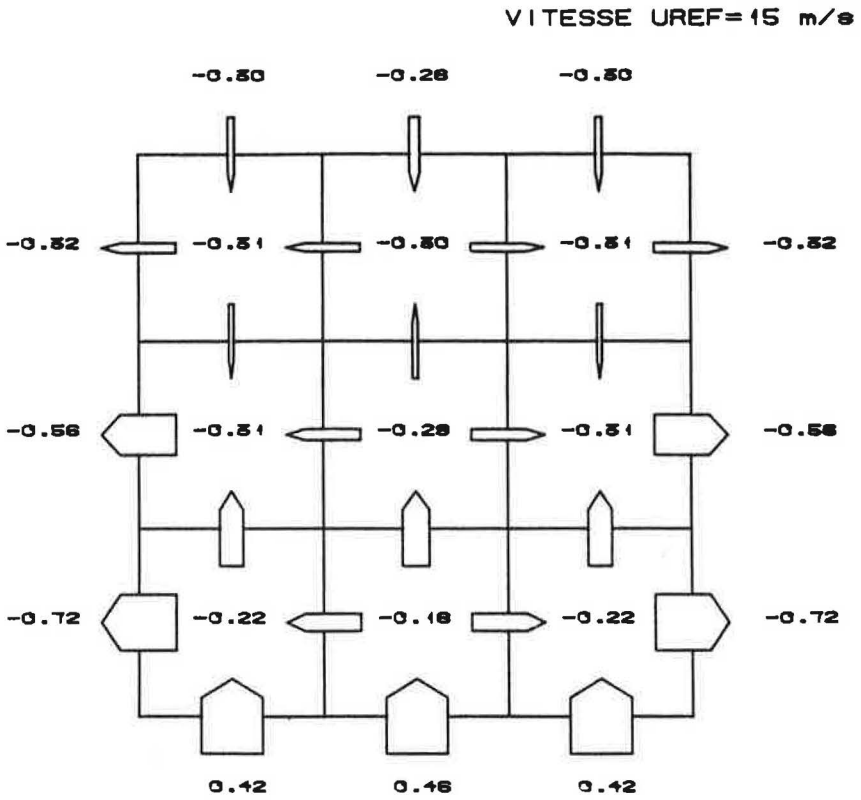

Fig. 6. The airflow distribution in a nine-zone system: Influence of opening dimensions, $\theta = 0^{\circ}$, $V = 15\ m/s, F_o = 9.10^{-2} m^2$

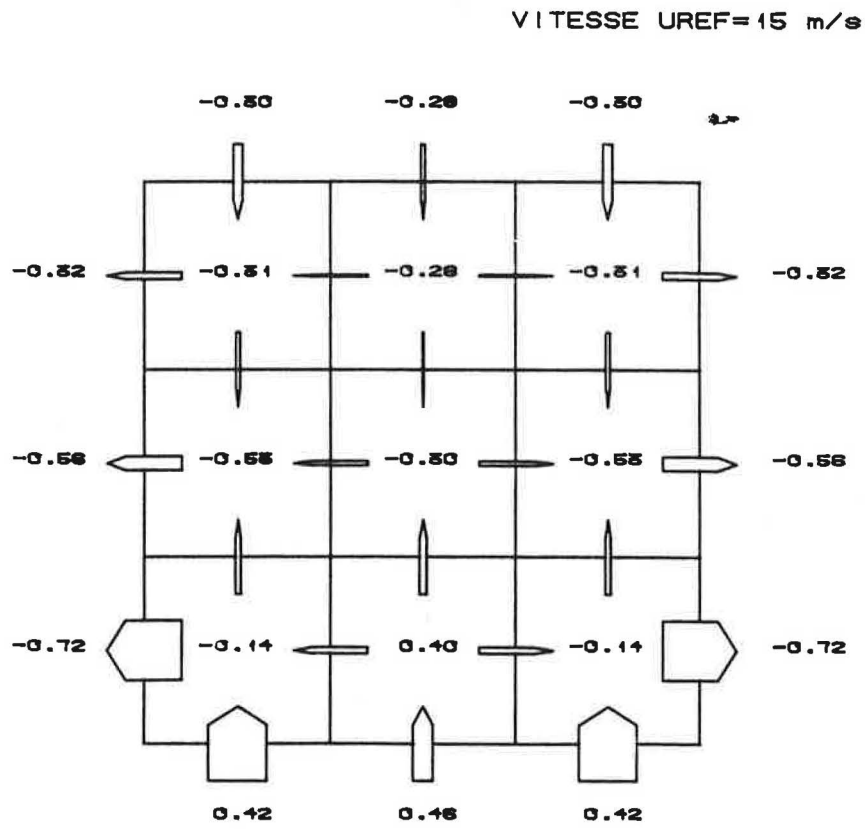

Fig. 7. The airflow distribution in a nine-zone system: Influence of inhomogeneous opening repartition, $\theta = 0^{\circ}$, $V = 15\ m/s, F_{oe} = 9.10^{-2} m^2$, $F_{oi} = 9.10^{-3} m^2$

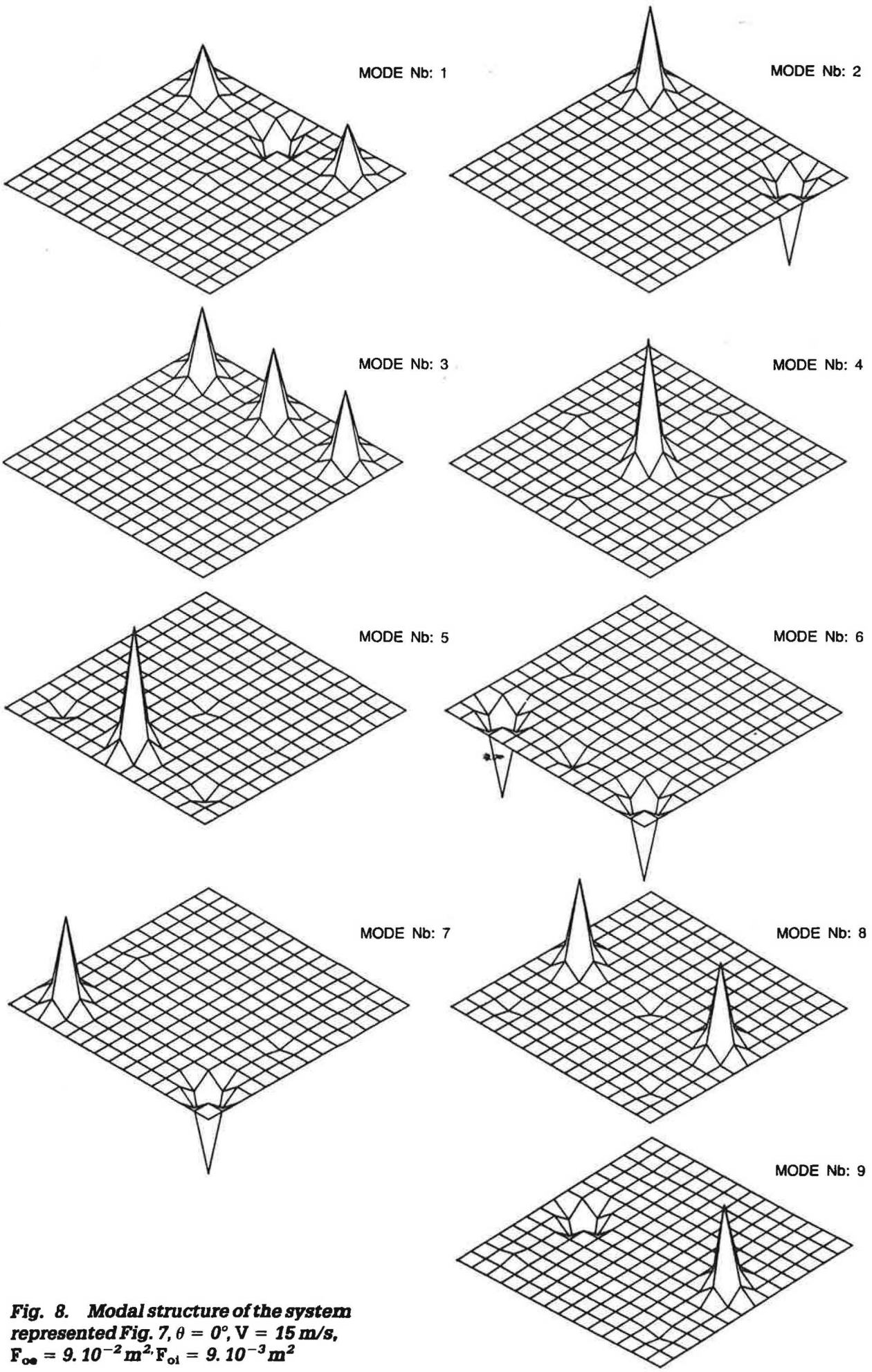

Fig. 8. Modal structure of the system represented Fig. 7, $\theta = 0°$, V = 15 m/s, $F_{oe} = 9.10^{-2} m^2$, $F_{oi} = 9.10^{-3} m^2$

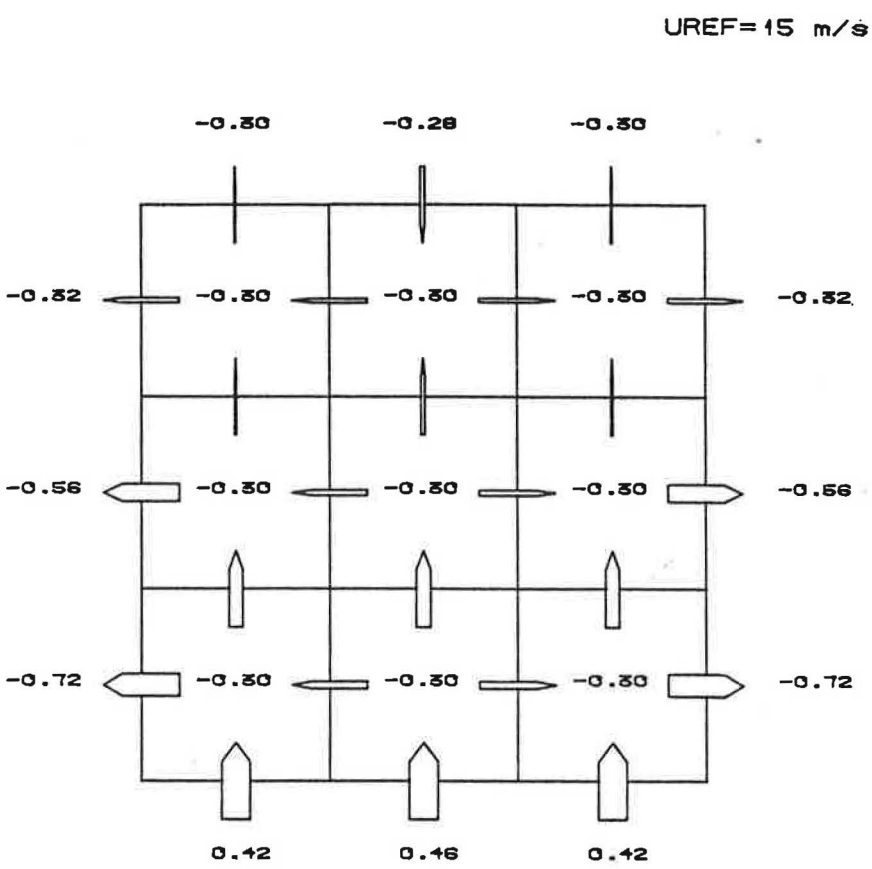

Fig. 9. The airflow distribution in a nine-zone system: Influence of inhomogeneous opening repartition, $\theta = 0°$, V = 15 m/s, $F_{oe} = 9.10^{-3} m^2$, $F_{oi} = 9.10^{-2} m^2$

Where $X \in R^m$, $U \in R^r$ and $Y \in R^q$, we require a reduced order model in the form of:

$$\begin{cases} FZ + GU = 0 \\ \hat{Y} = HZ + KU \end{cases} \tag{30}$$

where $Z \in R^{mr}$, $\hat{Y} \in R^q$ and $m_r < m$;

$$\begin{cases} FL = L\mathscr{A} \\ G = L\mathscr{B} \end{cases} \tag{31}$$

where L is the aggregated matrix.

The matrices F, G, H, K are chosen to minimize the quadratic error function:

$$J = (Y - \hat{Y})^T (Y - \hat{Y}) \tag{32}$$

The matrix F retains some of the eigenvalues of A. Suppose these eigenvalues belong to the bloc Λ_1 (Equation 23):

$$\Lambda = \begin{matrix} \\ mr\{ \end{matrix} \overset{mr}{\begin{bmatrix} \Lambda_1 & 0 \\ 0 & \Lambda_2 \end{bmatrix}} \qquad \Gamma = \begin{bmatrix} \Gamma_1 \\ \Gamma_1 \end{bmatrix} \} m_r$$

$$x^T = [x_1 \; x_2]^T$$

The more general aggregated model is given by:

$$\begin{cases} F = N \Lambda_1 N^{-1} \\ G = N \Gamma_1 \\ L = N [l_{mr} \mid 0] \, M^{-1} \end{cases} \tag{33}$$

with $L_0 = [l_{mr} \mid 0] \, M^{-1}$

Afterwards, we will take $N = I$ identity matrix.

The choice of modes is taken from a criterion of energy. From G. P. Michaïlesco's works (ref. 10), for each couple input-output i, j, each mode k energy contribution is given by $\mathscr{P}_{ij}(k)$, the k^{th} component of the line matrix $\mathscr{P}_{ij}$:

$$\mathscr{P}_{ij} = \Omega_j \otimes \Lambda^{-1} \Gamma_i$$

where Γ_i is the i^{th} column of Γ and Ω_j the j^{th} line of Ω.

In our case, we consider all inputs and outputs together. So we take the following formula:

$$\sum_{i=1}^{r} \sum_{j=1}^{q} r_i \, q_j \, \mathscr{P}_{ij}.$$

where r_i and q_j are weightings of inputs and outputs respectively ($r_i = U_i$ and $q_j = 1 \; \forall \, j$).

This energetic criterion allows us to classify system modes in order of importance. If we take K = $\mathscr{D}$ in the

output matrices H and K, the error minimization J (Equation 32) is calculated in relation to H:

$$J = \text{trace}\{(\mathscr{C} - HL_o)^T(\mathscr{C} - HL_o)\, W_O\}$$

$$\frac{\partial J}{\partial H} = 0 \qquad (34)$$

Equation 34 gives us:

$$H = \mathscr{C} W_0 L_0^T (L_0 W_0 L_0^T)^{-1} \qquad (35)$$

where $W_o = XX^T$

If the matrix $L_0 W_0 L_o^T$ can be inverted, these optimal conditions are also sufficient because:

$$\frac{\partial^2 J}{\partial h_j^2} = L_0 W_0 L_0^T > 0, \forall j = 1, \ldots, q.$$

where h_j denotes lines of H.

Reduction applications

Here we study some cases of reduction for the aeraulic model. We are going to examine wind incidence θ and opening repartition influences. To do that we choose a more realistic wind speed range of 6–8–10 m/s.

The aeraulic model and the aggregated model are compared by calculating the following remainders:

$$J_{\max} = \max\left[\frac{Y_i - \hat{Y}_i}{Y_j}\right]$$

$$\bar{J} = \left[\frac{1}{q}\sum_{j=1}^{q}\frac{(Y_i - \hat{Y}_i)^2}{Y_j^2}\right]^{1/2}$$

The principal stages of reduction are given in Appendix 3.

Wind incidence and reduction

a) Normal incidence $\theta = 0°$

The conditions of this example are: $m = 9$, V = 8 m/s, $F_{oe} = F_{oi} = 9.\ 10^{-3}\ m^2$

The energetic contributions for each mode are:

$\mathscr{P}(1) = 0.39\ 10^{-1}$	$\mathscr{P}(4) = 0.3.10^{-2}$	$\mathscr{P}(7) \simeq 10^{-18}$
$\mathscr{P}(2) = 0.33$	$\mathscr{P}(5) = 0.16$	$\mathscr{P}(8) = 0.4.10^{-2}$
$\mathscr{P}(3) \simeq 10^{-17}$	$\mathscr{P}(6) = 10^{-17}$	$\mathscr{P}(9) = 0.32$

After classifying the characteristic modes by decreasing energy order, we represent the flow rates for different states of reduction.

$m_r = 6$ (modes 2, 9, 5, 1, 8, 4)
$J_{\max} \simeq 10^{-11}$ $\bar{J} \simeq 10^{-6}$

(Figure 10)

$m_r = 3$ (modes 2, 9, 5)
$J_{\max} = 1{,}1$ $\bar{J} \simeq 4.3\%$

In this case the reduction is especially efficient and the aggregated model is a very good representation of the initial system.

b) Wind incidence $\theta = 45°$

In that case the conditions are: $m = 9$, $\theta = 45°$, $V = 6$m/s, $F_{oe} = F_{oi} = 9.\ 10^{-3}\ m^2$.

The external pressure distribution around building is given by R.M. Aynsley (ref. 4). Here the symmetry is broken and there is no more degeneration phenomenon. We give the energy distribution. Note that the results are equivalent for the modal analysis (ref. 7).

$\mathscr{P}(1) \sim 0.25$	$\mathscr{P}(4) \sim 0.27$	$\mathscr{P}(7) \sim 0.3.10^{-2}$
$\mathscr{P}(2) \sim 0.24$	$\mathscr{P}(5) \sim 0.11$	$\mathscr{P}(8) \sim 0.41$
$\mathscr{P}(3) \sim 0.7.10^{-2}$	$\mathscr{P}(6) \sim 0.5.10^{-2}$	$\mathscr{P}(9) \sim 0.16.10^{-1}$

The energy spectrum is much smaller, because the symmetry is broken.

$m_r = 6$ (modes 8, 4, 1, 2, 5, 9)
$J_{\max} = 120$ $J = 5\%$ (Fig. 11)

A reduction for normal incidence is better than a reduction at wind incidence $\theta = 45°$. Nevertheless the results are very satisfactory. The large value of $J_{\max}$ is due to errors made on small flow rates in the aggregated model.

Repartition of openings and reduction

We shall now study an example of a non-uniform repartition of openings. It is the same configuration compared with a normal incidence example ($m = 9$, $\theta = 0°$, $V = 6$ m/s, $F_{oe} = F_{oi} = 9.\ 10^{-3}\ m^2$) except for some permeabilities in zones 1, 4, 7 which are nil. Energy distribution is:

$\mathscr{P}(1) \sim 0.5\ 10^{-3}$	$\mathscr{P}(4) \sim 0.12\ 10^{-1}$	$\mathscr{P}(7) \sim 0.2\ 10^{-2}$
$\mathscr{P}(2) \sim 0.39$	$\mathscr{P}(5) \sim 0.17$	$\mathscr{P}(8) \sim 0.4\ 10^{-2}$
$\mathscr{P}(3) \sim 0.25\ 10^{-1}$	$\mathscr{P}(6) \sim 0.9\ 10^{-2}$	$\mathscr{P}(9) \sim 0.12$

In this case the symmetry is also broken.

$m_r = 6$ (modes, 2, 9, 5, 1, 8, 4)
$J_{\max} \simeq 3.4$ $J \simeq 4\%$ (Fig. 12)

These results show a good representation by the aggregated model.

Conclusions and future work

A realistic model has been developed which is able to represent air circulations in buildings. According to the terms of the study, the aeraulic behaviour modelling of buildings appears to be an essential tool.

First of all, we have synthesized the complexity of physics, while keeping a certain adaptability in the application of the AERA program. So we can test several configurations.

The modal structure analysis of the system has allowed us to understand better the relation between the given model and physics. In most cases, the former seems to be well represented by dominant characteristic modes of the system. So we have reduced this model. Among reduction techniques, we have chosen the linear aggregation method. The model reduction ability has been excellent at normal incidence (with a symmetrical repartition of openings) and also very good at a wind incidence $\theta = 45°$. The

a)

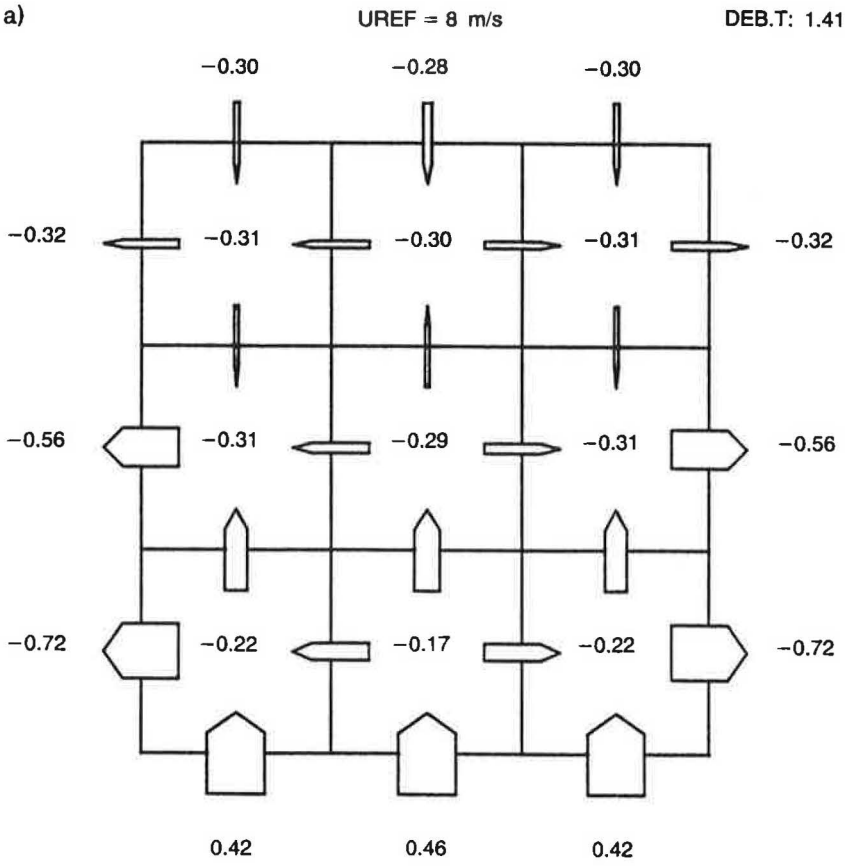

b)

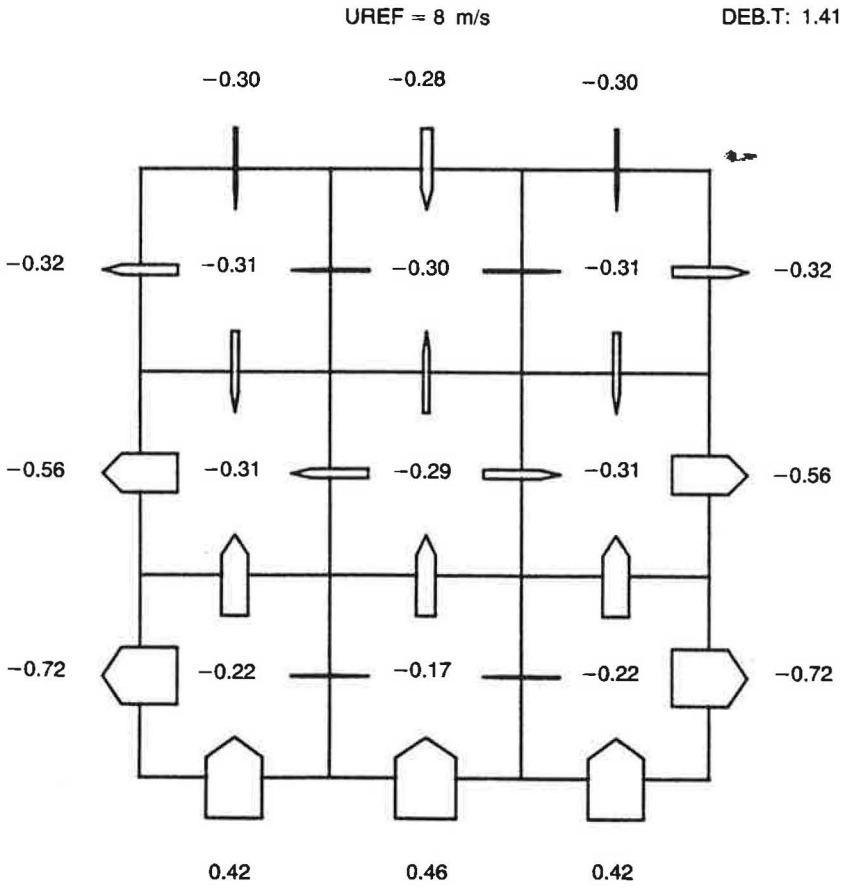

Fig. 10. Model reduction for an incidence $\theta = 0°$
a) V = 8 m/s mr = 6
b) V = 8 m/s mr = 3

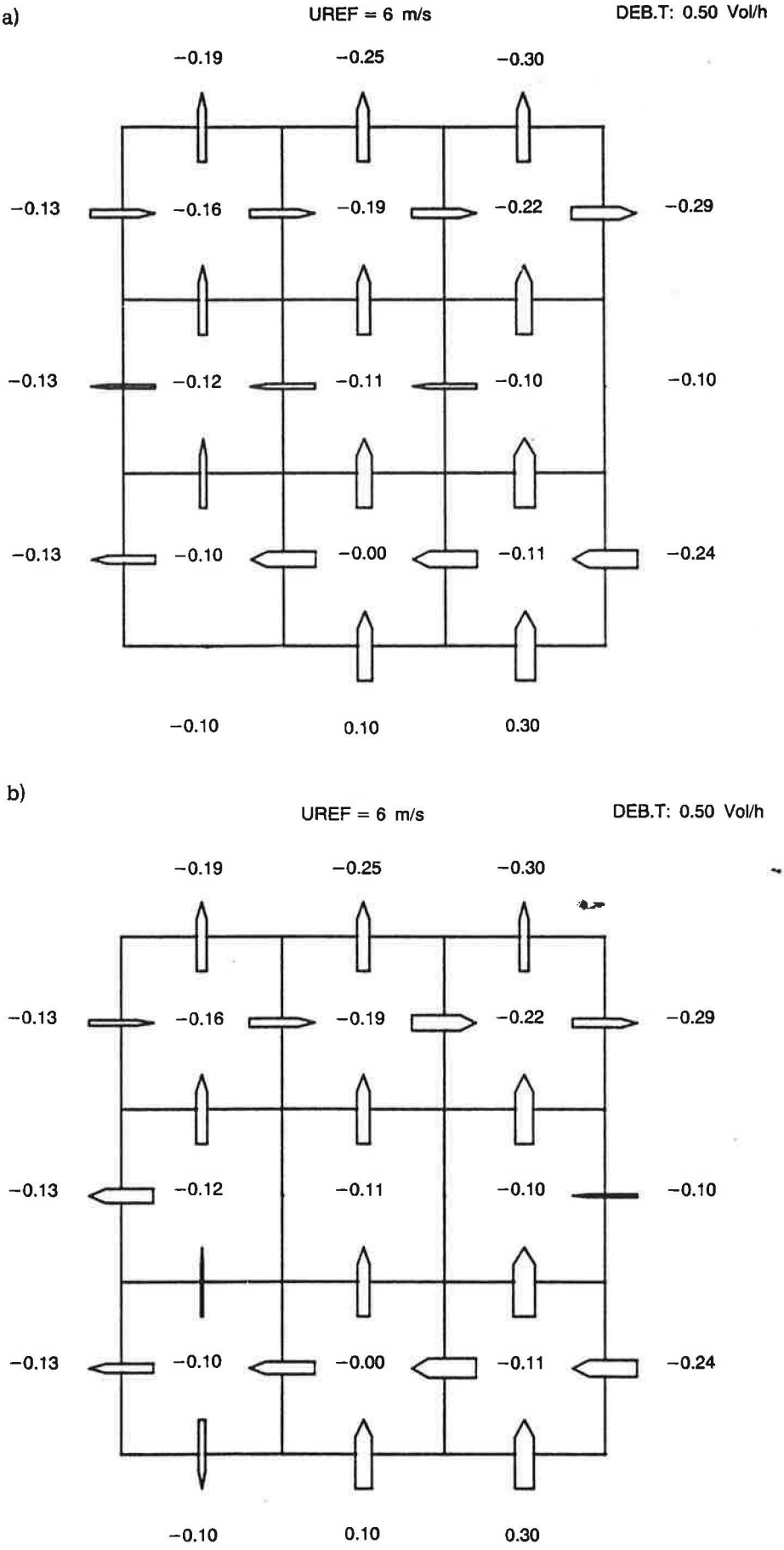

Fig. 11. The airflow distribution in a nine-zone system: Reducation for $\theta = 45°$, V = 6 m/s
a) initial model m = 9
b) reduced model mr = 6

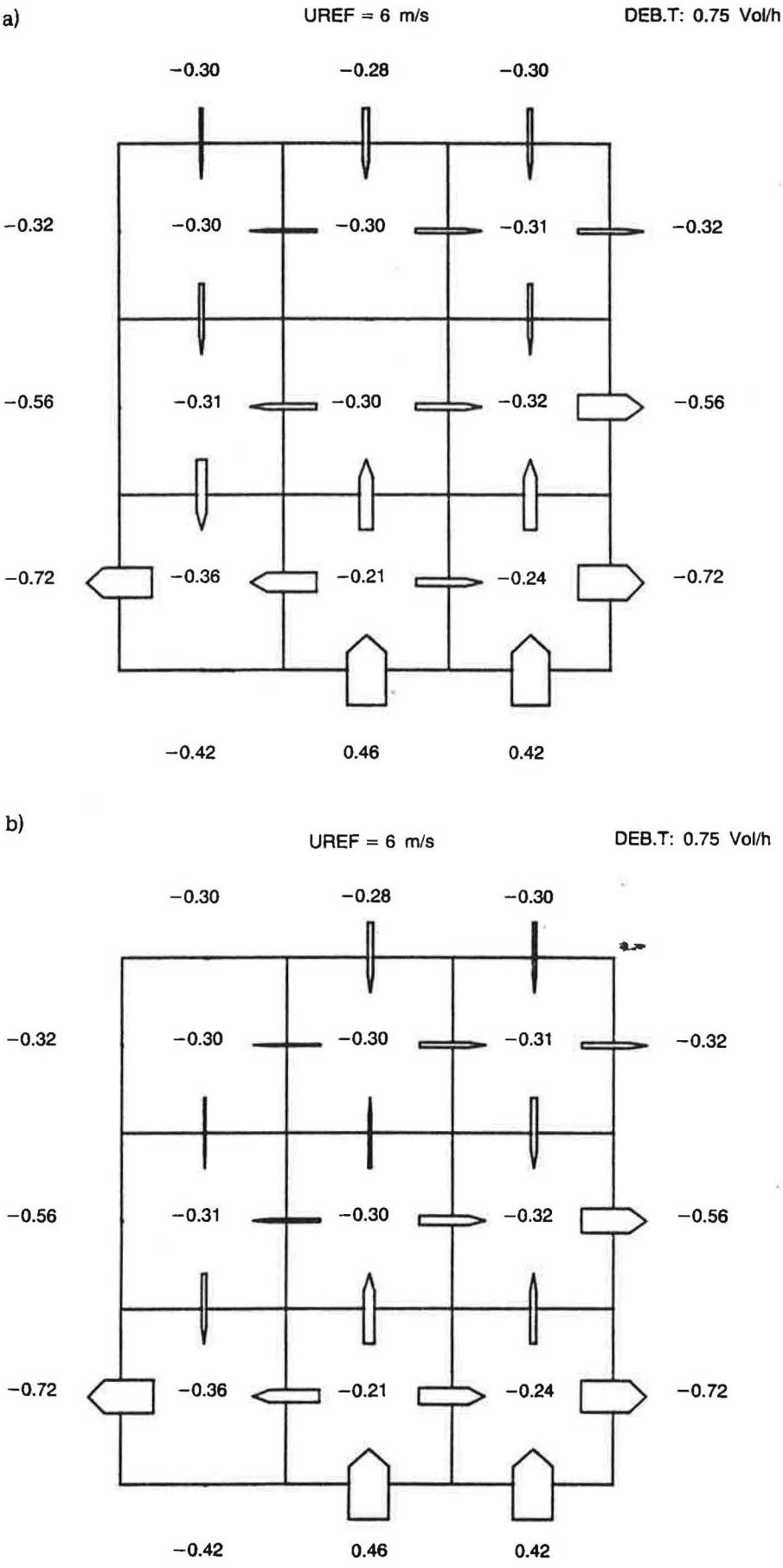

Fig. 12. The airflow distribution in a nine-zone system: non-uniform repartition of openings and model reduction $\theta = 0°, V = 6\ m/s, F_o = 9.10^{-3}\ m^2, \bar{R}(1,-2) = \bar{R}(4,3) = \bar{R}(7,6) = 0.$

a) initial model $m = 9$

b) reduced model $mr = 6$

results have been good for non-symmetrical repartition of openings.

Coupling this aeraulic model with a more general heat housing simulation has been one of our principal aims. In this way, heat engineers of buildings can improve the evaluation of heat transfers due to aeraulic phenomena. In the event of a coupling, the model reduction can be interesting with systems of large dimensions.

Appendix 1

Calculation of permeability function (ref. 5)

Now we are going to develop the description of discharge through an opening, given by the Memento des pertes de charge (ref. 5).

In the case of flow through orifices in pipes, we recall that different results should be expected for discharge through building openings (ref. 4).

In 'Memento' the flow is characterized by air speeds and crossing-areas as: w_1, F_1 for flow before opening, w_o, F_o through opening, w_2, F_2 after opening.

For a real discharge, because of losses through opening, the drop in pressure is given as:

$$\Delta P = 0.5\,\xi\,\rho\,V^2 \qquad \text{(A.1)}$$

$\xi \geqslant 1$ is called drop in pressure coefficient.
From the flow definition $Q = K\Delta P$, the permeability expression is obtained as:

$$K = 2F_o^2/\xi\,\rho Q \qquad \text{(A.2)}$$

From the expression of ξ we can see how the permeability depends on flow rate through opening. Indeed ξ depends on geometric characteristics and also on the Reynolds number which characterizes the type of flow through opening.

1) $Re > 10^5$ (Turbulent flow)

$$Re = \rho\, w_o\, D_o/\mu = \rho\, QD_o/F_o\mu$$

ρ: air density
μ: dynamic viscosity of air
D_o: hydraulic diameter of opening

with $D_o = \dfrac{4F_o}{\pi_o}$, π_o: perimeter

$$\xi = 0.5(1 - F_o/F_1) + (1 - F_o/F_2)^2 + \tau\sqrt{1 - F_o/F_1}\,(1 - F_o/F_2) + \lambda\frac{1}{D_o} \qquad \text{(A.3)}$$

$$\xi = \xi_o + \lambda\frac{1}{D_o}$$

where τ is given by the curve $\tau = f(1/D_o)$ (Fig. A.2).

The expression $\lambda l/D_o$ represents the linear drop in pressure through opening, which is negligible in relation to singular drop in pressure ξ_o. This later only depends on geometric characteristics:

$$\xi_o = 0.5(1 - F_o/F_1) + (1 - F_o/F_2)^2 + \tau\sqrt{1 - F_o/F_1}\,(1 - F_o/F_2)$$

2) $Re < 10^5$

$$\xi = \zeta\phi + \varepsilon^{Re}{}_o\,\xi_o \qquad \text{(A.4)}$$

ζ_ψ and $\varepsilon^{Re}{}_o$ are given in Figure A.3.

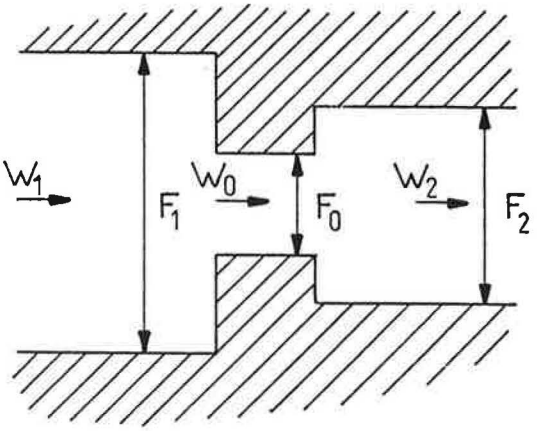

Fig. A.1. Section of an opening letting the airflow through from one volume to another

ζ_φ characterizes the singular aspect of flow with the ratio F_o/F_1. Indeed the more important the ratio, the more the flow is disturbed in crossing the opening. This phenomenon is less important when Re increases. The discharge is more sensitive to geometric variations at small speeds than at large speeds. In that case the linear drop in pressure through opening is neglected.

We have to remember the reservations made earlier about the results of Memento. In our work the drop in pressure function ξ has been selected and a linear drop in pressure into each zone has been added.

In direction of flow:

$$\zeta_l = \xi_1{}^*\, L/D_h \qquad \text{(A.5)}$$

ξ_1 essentially depends on Re:

$\xi_1 = 0.316 \times Re^{-1/4}$ law of Blasius (turbulent)
$\xi_1 = 64/Re$ (laminar)

In conclusion we can write:

$$K = 2F_0/[\xi + (\xi_1{}^*\, L/D)]\rho Q$$
$$Re = \rho\, QD_o/F_o\,\mu \rightarrow \xi$$
$$Re = \rho\, QD_h/F_2\,\mu \rightarrow \xi_1$$

Appendix 2

Description of application program area

The equations (7–15) of the system in steady state are numerically solved:

$$\underbrace{Y_i \rightarrow \bar{R}_i \rightarrow (A, B, C, D)_i \rightarrow X_i \rightarrow Y_{i+1}}_{\text{test of convergence}}$$

From a flow rate vector Y assumed to be surrounding the solution, the calculation of permeabilities allows to determine the matrices A, B, C, D which permit the calculation of state vector X and the new output vector Y, and so on. This is the iterative method of Newton.

For the calculation of state vector X, we have inversed the matrix A by the method of 'Elimination de Gauss avec recherche du pivot partiel', chosen in HARWELL Library of solution programs. This method gives a good precision in calculations.

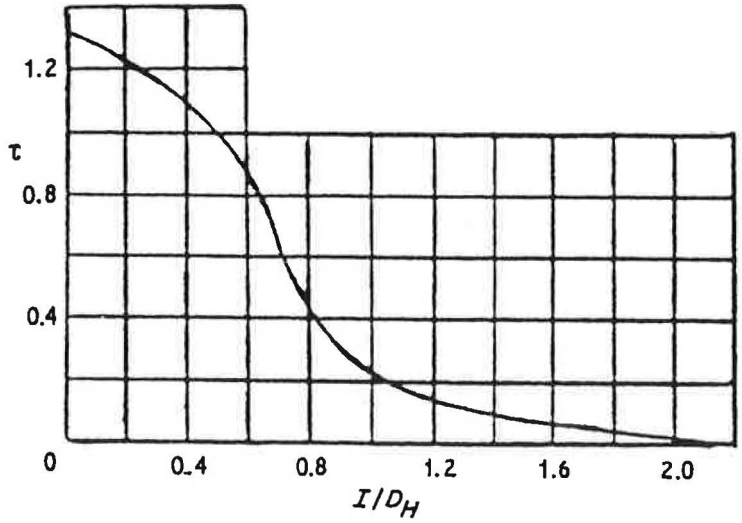

I/D_H	τ	I/D_H	τ
0	1.35	1.0	0.24
0.2	1.22	1.2	0.16
0.4	1.10	1.6	0.07
0.6	0.84	2.0	0.02
0.8	0.42	2.4	0

Fig. A.2. τ function of the opening geometric characteristics (ref. 5)

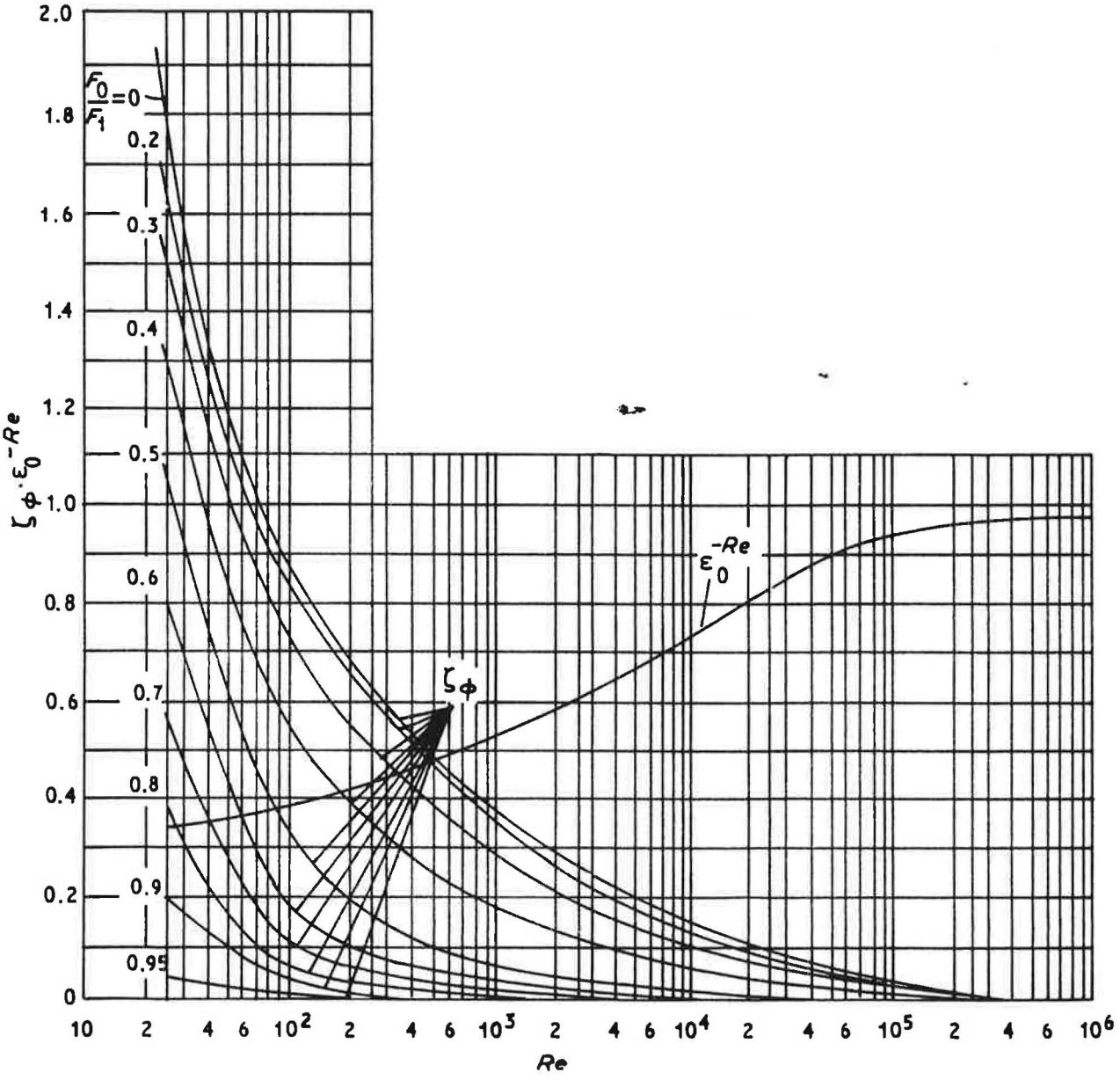

Fig. A.3. Description of drop in pression functions ε_o^{Re} and ζ_ϕ

Begin

- Give the parameters of system.
- Open files where the results are stocked.
- Standard data for the permeability calculation.

- Do you want to change dimensions of one or several zones and/or openings?
  If Yes ***then*** Give the new dimensions of zones and/or openings ***Endif***

  If dimension of system equals 1 ***then***
  Call the subroutine MONO
  Exit
  Endif

- How many cases do you want IN = ?

- Do you want to change the external pressure distribution?
  If Yes ***then*** Give the new pressure distribution
  Endif

Do For IS = 1 to IN

- Case number NE = ?
- Reference wind speed V = ?
- Begin of the iterative calculation.

Do while (stop iterative calculation = False)

- For each number of iterations which is a multiple of 10, reduce the coefficient α of 10% for improving the convergence.
- Call the subroutine FON for calculating the permeabilities.
- Calculate the matrices A, B, C, D.
- Calculate the characteristic values of A.
- Calculate the state vector X in steady state.
- Calculate the flow rate vector Y in steady state.
- Sub-relaxation for improving the speed of convergence in the method of Newton: $Y_{i+1} = \alpha\, Y_{i+1} + (1-\alpha)\, Y_i$

End do

- Stock the results in files

End do

- For a speed range we can calculate the linear system.

If (IN $\geq$ 2) ***then***

- Calculate the linear matrices $\mathscr{A}$, $\mathscr{B}$, $\mathscr{C}$, $\mathscr{D}$.
- Calculate the vectors X and Y of the system:
  $$\begin{cases} \mathscr{A}X + \mathscr{B}U = 0 \\ Y = \mathscr{C}X + \mathscr{D}U \end{cases}$$
- Compare the linear system with the initial system.

Endif

END

Appendix 3

Description of reduction

Begin

- Parameters of system.
- Taking the results of the program AERA.
- Calculation of the matrix W_o.
- (Reduce = true; Energy = false).
- ***Do while*** (reduce = true)

  If (Energy = False) *Then*

  - Calculate $\mathscr{P}$ matrix of energy associated to each mode.
  - Classify the characteristic values in order of $P(k)$ decreasing.

  End if

  - Do the choice of eigenvalues.
  - Calculate $H = \mathscr{C}.W_0.L_0^T\,(L_{0.W0}.L_0^T)^{-1}$
  - Calculate the outputs $\hat{Y}$ of the reduced model

    $$\hat{Y} = HX + \mathscr{D}U$$

    Compare Y and $\hat{Y}$:

    $$J_{\max} = \max \left[\frac{Y_i - \hat{Y}_i}{Y_j} \right]$$

    $$j = \left[\frac{1}{q} \sum_{j=1}^{q} \frac{(Y_i - \hat{Y}_i)^2}{Y_j^2} \right]$$

  - Energy = true
  - Would you reduce again?
  - *If* yes *then*
    reduce = true
    else reduce = false
  - ***End If***

End do

End

References

1. Evans, B.H. (1979) 'Energy conservation with natural airflow through windows', Ashrae Transaction, 85 (2).
2. Lee, B.E. (1977) 'Aerodynamic effects of building groups', Proceedings of the sixth course airflow and building design, Department of Building Science, Sheffield University, January.
3. Gandemer, J. and Guyot, A. (1976) 'Integration du phénomène dans la conception du milieu bâti', La documentation française.
4. Aynsley, R.M. (1977) 'A study of airflow through and around buildings', PhD Thesis, University of New South Wales, School of Buildings, Australia.
5. Idel'Cik (1979) 'Memento des pertes de charge', Paris.
6. Barnaud, G. and Gandemer, J. 'Détermination en soufflerie simulant le vent naturel, des coefficients de pression externe sur une tour d'habitation et un hall industriel', CSTB de Nantes, En Adym 75-9-R.
7. Passard, J. (1989) 'Etude des écoulements d'air dans l'habitat: Modélisation, application à la thermique du bâtiment', Thèse de l'Université de Paris VII, Février.
8. Aoki, M. (1968) 'Control of large scale dynamic systems by aggregation', IEEE Transaction on automatic control, Vol. AC-13, No 3, June.
9. Michailesco, G. and Duc, G. 'L'approche de la réduction des modèles en automatique: Classification des principales méthodes', Laboratoire des signaux et systèmes, service automatique.
10. Michailesco, G.P. (1979) 'Approximation des systèmes complexes par des modèles de dimension réduite', Thèse d'Etat présentée au Centre d'Orsay, Paris Sud. Avril.